JACC: CARDIOVASCULAR IMAGING
VOL. 11, NO. 1, 2018
© 2018 BY THE AMERICAN COLLEGE OF CARDIOLOGY FOUNDATION
ISSN 1936-878X/$36.00
PUBLISHED BY ELSEVIER
http://dx.doi.org/10.1016/j.jcmg.2017.02.014

Intervendor Differences in the Accuracy of Detecting Regional Functional Abnormalities

A Report From the EACVI-ASE Strain Standardization Task Force

Oana Mirea, MD, PhD,[a] Efstathios D. Pagourelias, MD, PhD,[a] Jurgen Duchenne, MSc,[a] Jan Bogaert, MD, PhD,[b] James D. Thomas, MD,[c] Luigi P. Badano, MD, PhD,[d] Jens-Uwe Voigt, MD, PhD,[a] on behalf of the EACVI-ASE-Industry Standardization Task Force

ABSTRACT

OBJECTIVES The purpose of this study was to compare the accuracy of vendor-specific and independent strain analysis tools to detect regional myocardial function abnormality in a clinical setting.

BACKGROUND Speckle tracking echocardiography has been considered a promising tool for the quantitative assessment of regional myocardial function. However, the potential differences among speckle tracking software with regard to their accuracy in identifying regional abnormality has not been studied extensively.

METHODS Sixty-three subjects (5 healthy volunteers and 58 patients) were examined with 7 different ultrasound machines during 5 days. All patients had experienced a previous myocardial infarction, which was characterized by cardiac magnetic resonance with late gadolinium enhancement. Segmental peak systolic (PS), end-systolic (ES) and post-systolic strain (PSS) measurements were obtained with 6 vendor-specific software tools and 2 independent strain analysis tools. Strain parameters were compared between fully scarred and scar-free segments. Receiver-operating characteristic curves testing the ability of strain parameters and derived indexes to discriminate between these segments were compared among vendors.

RESULTS The average strain values calculated for normal segments ranged from −15.1% to −20.7% for PS, −14.9% to −20.6% for ES, and −16.1% to −21.4% for PSS. Significantly lower values of strain ($p < 0.05$) were found in segments with transmural scar by all vendors, with values ranging from −7.4% to −11.1% for PS, −7.7% to −10.8% for ES, and −10.5% to −14.3% for PSS. Accuracy in identifying transmural scar ranged from acceptable to excellent (area under the curve 0.74 to 0.83 for PS and ES and 0.70 to 0.78 for PSS). Significant differences were found among vendors ($p < 0.05$). All vendors had a significantly lower accuracy to detect scars in the basal segments compared with scars in the apex ($p < 0.05$).

CONCLUSIONS The accuracy of identifying regional abnormality differs significantly among vendors.
(J Am Coll Cardiol Img 2018;11:25–34) © 2018 by the American College of Cardiology Foundation.

From the [a]Department of Cardiovascular Diseases, University Hospital Leuven, Leuven, Belgium; [b]Department of Radiology, University Hospital Leuven, Leuven, Belgium; [c]Bluhm Cardiovascular Institute, Northwestern University, Chicago, Illinois; and the [d]Cardiac, Thoracic and Vascular Sciences, University Padua, Padua, Italy. Dr. Mirea is permanently affiliated to the Department of Cardiology, University Hospital of Craiova, Romania. This study was supported by a dedicated grant from the American Society of Echocardiography. Dr. Mirea has received a research grant from the European Association of Cardiovascular Imaging. Dr. Pagourelias holds a research grant from the European Association of Cardiovascular Imaging. Dr. Thomas has received honoraria and consulting fees from Edwards Lifesciences, Abbott, and GE. Dr. Voigt holds a personal research mandate from the Flemish Research Foundation; and has received a research grant from the University Hospital Gasthuisberg. All other authors have reported that they have no relationships relevant to the contents of this paper to disclose.

Manuscript received October 21, 2016; revised manuscript received January 24, 2017, accepted February 17, 2017.

JACC: CARDIOVASCULAR IMAGING, VOL. 11, NO. 1, 2018
JANUARY 2018:25–34

ABBREVIATIONS AND ACRONYMS

AUC = area under the curve

AVC = aortic valve closure

CMR = cardiac magnetic resonance

ES = end-systolic

LGE = late gadolinium enhancement

LV = left ventricle

MI = myocardial infarction

PS = peak systolic

PSI = post-systolic index

PSS = post-systolic strain

ROC = receiver-operating characteristic

The accurate noninvasive evaluation of regional myocardial function is essential in clinical practice. In heart failure patients with conduction delays, myocardial function can differ significantly between walls, and its accurate assessment could be of potential use for selecting suitable candidates for resynchronization therapy, which would have implications for therapy success and survival (1). After myocardial infarction (MI), the early detection of ischemic injury and the evaluation of myocardial viability directly determines patient management and can prevent serious complications such as sudden cardiac death, left ventricular (LV) remodeling, or arrhythmias (2–4).

In clinical cardiology, cardiac ultrasound is the method of choice for the noninvasive evaluation of regional LV function. In clinical practice, the assessment of regional function abnormalities still relies mostly on the visual interpretation of wall motion abnormalities, which makes it subjective and dependent on skills and experience.

SEE PAGE 35

Two-dimensional speckle tracking echocardiography allows the objective quantification of LV global and regional function in a convincingly simple and feasible way. The method has been validated against sonomicrometry and cardiac magnetic resonance (CMR) (5), and global longitudinal strain has proved to be a clinically reliable and reproducible parameter of LV systolic function (6). Likewise, segmental strain measurements have been shown to detect the presence and extent of ischemia (7–13) and distinguish between viable and nonviable myocardial segments (14), which makes them a potential alternative to the conventional "eye-balling" analysis. It is not clear, however, whether current tracking software is sufficiently accurate for this and to what extent the performance of software from different vendors differs.

The present study was designed to evaluate and compare in a clinical setting the accuracy of different software packages to detect regional functional abnormality.

METHODS

STUDY POPULATION. Sixty-three patients, age >18 years, with regular heart rhythm and a previous MI were selected for the study. In all patients, a late gadolinium enhancement (LGE) CMR study had been performed after an MI (without other ischemic events or cardiac interventions before the image acquisitions for this study). Five patients had to be replaced by healthy young volunteers who were on stand-by because of no-show or paroxysmal atrial fibrillation. The study was approved by the ethics commission of the University Hospitals Leuven, and all subjects gave written informed consent before inclusion.

INDUSTRY PARTNER RECRUITMENT. Seven industry partners (Hitachi, Tokyo, Japan; Esaote, Florence, Italy; GE Vingmed Ultrasound, Horten, Norway; Philips, Andover, Massachusetts; Samsung, Seoul, South Korea; Siemens, Mountain View, California; and Toshiba, Otawara, Japan) provided an ultrasound machine, post-processing software, and an application specialist responsible for optimizing the machine settings according to requirements for speckle tracking analysis. Additionally, 2 manufacturers of generic software solutions for speckle tracking analysis (Epsilon, Ann Arbor, Michigan and TOMTEC, Unterschleissheim, Germany) participated in the comparison. One company withdrew from the study for technical reasons. A list of participants and the versions of software used for analysis is provided in Table 1.

STUDY PROTOCOL. Echocardiographic imaging. The echocardiographic image acquisitions were completed in 5 days during 9 sessions of 2 to 3 h each. Each patient was scanned by an expert examiner. Seven patients were examined per session each by 1 expert echocardiographer on all 7 ultrasound machines. Application specialists from all companies ensured optimal machine settings during the scans. Images were obtained with the subject in the left lateral decubitus position. Three consecutive cardiac cycles from the apical views (4-, 2-, and 3-chamber) were obtained during breath hold. Additionally, pulsed wave Doppler recordings of the mitral inflow and aortic outflow were acquired for timing measurements. All image data were stored as raw data in a proprietary company format and in the standard DICOM (Digital Imaging and Communications in Medicine) format to allow post-processing with the independent software packages.

CMR imaging. All patients had undergone a CMR study on a 1.5-T Philips Intera-CV (Philips, Best, the Netherlands) using dedicated cardiac software, a phased-array surface receiver coil, and electrocardiography triggering. The CMR acquisitions were performed no sooner than 4 days after the MI. Cine images in horizontal, vertical, and short-axis views were acquired using a breath-hold cine steady-state free-precession sequence. Post-contrast breath-hold T1-weighted 3-dimensional inversion-recovery

imaging was used for detection and quantification of LGE 10 min after intravenous bolus of 0.2 mmol/kg gadolinium-tetraazacyclododecane-tetraacetic acid (Dotarem, Guerbet, Villepinte, France), with the same views that were used for cine images. The inversion time was individually adapted to suppress the signal of normal myocardium (220 to 350 ms). Extent and transmurality of scar were documented per segment using the standard 18-segment model recommended for functional echocardiographic measurements (15).

DATA ANALYSIS. Conventional echocardiography. LV ejection fraction was measured on GE images using the modified Simpson rule (15). Myocardial scar was visually assessed in the 2-dimensional images of each ultrasound machine using an LV 18-segment model and the following criteria: 1) thinned wall; 2) hypokinesia or akinesia; and 3) increased reflectivity of the myocardium. For the 2 independent software tools, scar readings from 1 vendor (GE) were used.

Speckle tracking echocardiography. Images were analyzed by a single observer (O.M.). All strain measurements were performed on vendor-specific speckle tracking software. For the 2 independent software providers, DICOM images acquired with the GE system were used. For all strain analysis, the LV was divided into 18 segments, as recommended for regional function analysis (15).

End diastole was manually set as the R peak of the electrocardiogram. If the software did not allow that, the automatic settings of the software were used instead. Aortic valve closure (AVC) was calculated from the pulsed wave Doppler recordings of the LV outflow. The endocardial borders were traced manually whenever possible. Otherwise, the region of interest was created by automated recognition according to the requirements of the respective software.

Tracking accuracy of the different software solutions was assessed visually. Segments were excluded from further analysis when the tracking did not accurately follow the underlying myocardial motion after at least 2 attempts to readjust the region of interest. Because we had 2 sets of apical views from each vendor, we used the datasets with the best image quality for the scar detection analysis. Feasibility of strain measurements, however, was calculated considering both acquisitions (2,268 segments per vendor).

Strain measurements. Zero strain was defined at end diastole as described above. For each segmental strain curve, peak systolic strain (PS), end-systolic strain (ES), and the post-systolic strain (PSS) peak were measured. The peaks were defined as follows: PS, maximum (positive or negative) strain value before AVC; ES, strain value at AVC; and PSS, maximum negative deformation after AVC, if more negative than ES (Figure 1). Additionally, the post-systolic index (PSI) was calculated as: (PSS − ES)/PSS × 100.

TABLE 1 Vendors Participating in the Study With Type and Version of Equipment Provided

Vendor	Ultrasound Machine	Type	Software and Version
Hitachi	ProSound F75	High end	2DTT Analysis v6.0
Esaote	MyLabAlpha eHD	Portable	XStrain2D v5.50
GE	Vivid E9	High end	EchoPAC v20.1
Philips	EPIQ	High end	*
Samsung	RS80A with Prestige	High end	Kardia 1.00.0615
Siemens	ACUSON S2000 CV system	High end	syngo VVI v4.0
Toshiba	Artida	High end	ACP v3.2
Epsilon†			EchoInsight
TOMTEC†			2D CPA 1.3 (module of TOMTEC-Arena)

*Prototype software withdrawn for technical reasons. †Software-only vendor.
2D = 2-dimensional; CPA = cardiac performance analysis.

CMR analysis. The CMR images were analyzed by consensus of 2 observers (O.M., E.D.P.). The readings were supervised by a CMR specialist (J.B.). We used an 18-segment model of the LV. Segmentations of CMR and echocardiographic datasets were carefully aligned by use of anatomic landmarks such as papillary muscles or the intersection of the right ventricular free wall with the interventricular septum. The presence of LGE was visually assessed from 3 short-axis projections (base, midventricular, apex) representing the middle of the echocardiographic segment.

Segments were rated as "nontransmural scar" when 1% to 75% of the segment showed hyperenhancement in the transmural direction; otherwise, they were labeled as "no scar" or "transmural scar." Segments were rated as "partial scar" when >20% but <80% of the segment showed hyperenhancement in the circumferential or longitudinal direction. Although no CMR was available, all segments from healthy volunteers were assigned a no-scar status for the statistical analysis.

For comparison with echocardiography data, we exclusively used segments with no scar and transmural scar. Therefore, in the following, the term *scarred segment* will be used in the sense of transmural scar, unless explicitly stated otherwise.

The healthy volunteers did not undergo CMR. The 90 segments analyzed from the volunteers were included in the final analysis as no scar.

STATISTICAL ANALYSIS. We used SPSS version 23.0 (SPSS Inc., Chicago, Illinois) for statistical analysis. The normal distribution of the data was tested with the Kolmogorov-Smirnov test. Continuous variables are expressed as mean ± SD. Comparison of

FIGURE 1 Schematic of How Longitudinal Strain Curves Were Analyzed

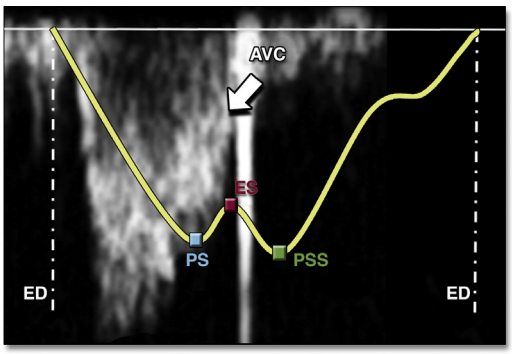

In the background, a spectral Doppler flow profile of the aortic valve with a marked closure artifact (AVC) is shown. The strain curve is represented in **yellow**. **White dashed lines** indicate the timing of the R peak in the electrocardiogram, which was used as a surrogate of ED and which defined zero strain. ED = end diastole; ES = end-systolic strain, measured at the time of aortic valve closure; PS = peak systolic strain, defined as positive or negative peak during systole; PSS = post-systolic strain, any peak more negative than end-systolic strain after aortic valve closure.

strain values between scarred and normal segments was performed with a 2-tailed Student *t* test. A p value <0.5 was considered significant. Receiver-operating characteristic (ROC) curves for PS, ES, PSS, and PSI were calculated to evaluate the discrimination capacity between normal segments and scars for each vendor. Area under the curve (AUC) of ROC was interpreted as follows (16): 1) AUC = 0.5, no discrimination; 2) 0.6 ≤ AUC < 0.7, poor discrimination; 3) 0.7 ≤ AUC < 0.8, acceptable discrimination; 4) 0.8 ≤ AUC < 0.9, excellent discrimination; and 5) AUC > 0.9, outstanding discrimination. The comparison between ROCs was performed with a De Long test (17) (MedCalc Software, Mariakerke, Belgium).

FIGURE 2 Distribution of Segments With No Scar, With Nontransmural or Partial Scar, and With Transmural Scar per Myocardial Level (Base, Midventricular, and Apical) as Defined by CMR LGE

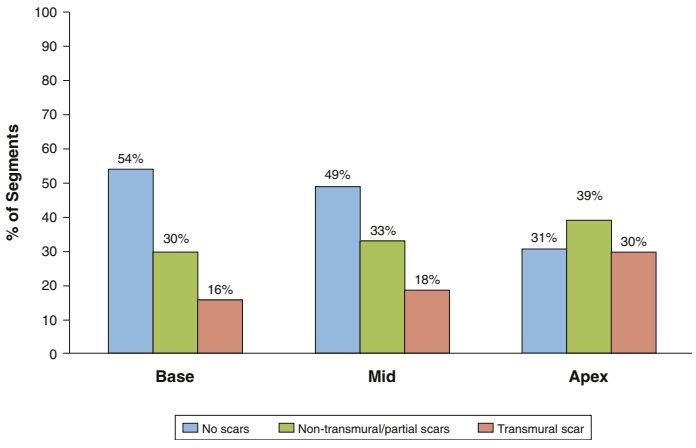

Segments with transmural scar were most prevalent in the apex. CMR = cardiac magnetic resonance; LGE = late gadolinium enhancement.

RESULTS

CONVENTIONAL ECHOCARDIOGRAPHIC PARAMETERS. Ejection fraction ranged from 28% to 75% (mean 54 ± 10%).

CMR ANALYSIS. The CMR examinations were performed on average 12 ± 8 months before the study and no sooner than 4 days after the MI. Of 1,044 segments analyzed, 241 had a transmural scar (23%). No LGE was present in 658 (63%) of the segments. The remaining 145 segments (14%) had nontransmural or partial scar. An average of 5.0 segments with transmural scar per patient (28% of the total myocardium) were present on LGE readings. Transmural scar was most prevalent in the apex (one-third of the apical segments) (**Figure 2**).

FEASIBILITY OF STRAIN ANALYSIS. The feasibility of segmental strain measurements ranged from 77.1% to 92.9% and differed significantly between vendors (ANOVA p < 0.05) (Online Figure 1).

STRAIN MEASUREMENTS. The average strain values calculated for normal segments ranged from −15.1% to −20.7% for PS (**Figure 3**), −14.9% to −20.6% for ES, and −16.1% to −21.4% for PSS (Online Figures 2 and 3). Significant differences were found among vendors (ANOVA, p < 0.05). The scarred segments had lower strain values for all vendors (p < 0.05), with average values ranging from −7.4% to −11.1% for PS, −7.7% to −10.8% for ES, and −10.5% to −14.3% for PSS (**Figure 3 and** Online Figures 2 and 3, respectively). Also here, significant differences were found among vendors (ANOVA, p < 0.05). The highest difference of PS strain between normal and scarred segments was 11.8% (GE) and the lowest 7.7% (Esaote, Toshiba). The respective data for ES and PSS are displayed in Online Figures 2 and 3.

Post-systolic shortening was found in both normal and scarred segments for all vendors. However, the PSI differed significantly between normal and scarred segments (p < 0.01) (**Figure 4**).

DISTINCTION OF SEGMENTS WITH AND WITHOUT SCAR. The ROC analysis for the ability of PS, ES, and PSS to distinguish segments with and without scar is shown in **Figure 5**. AUCs differed significantly among vendors (p < 0.05). The discrimination capacity was acceptable to excellent, with AUCs ranging from 0.74

FIGURE 3 **Average Values of PS Strain in Segments Without Scar and With Transmural Scar**

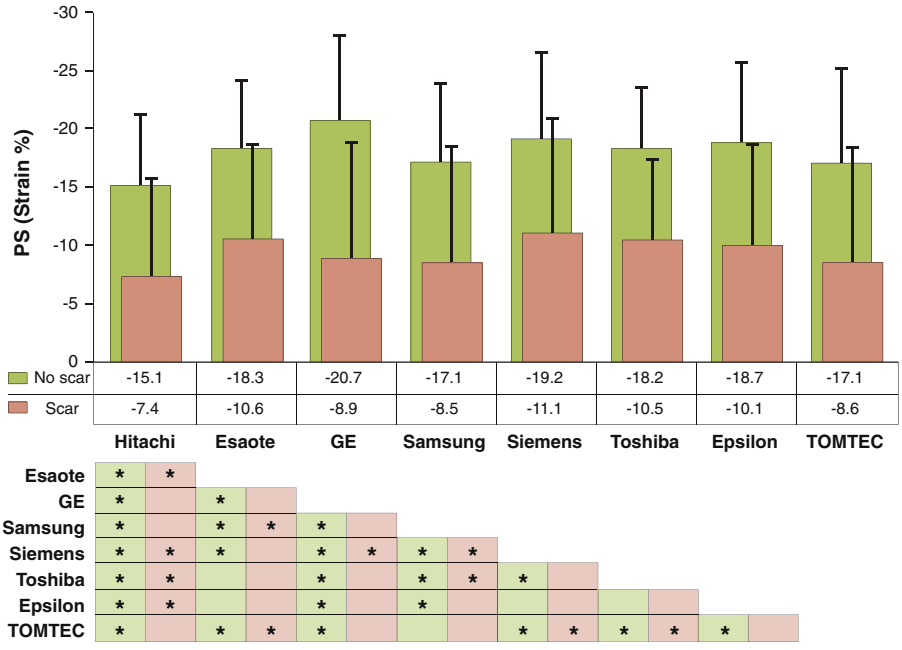

The table immediately below the Figure displays the respective post hoc tests for strain difference, *p value <0.05 among vendors. The strain difference differed considerably among vendors (ANOVA, $p < 0.05$). Abbreviations as in Figure 1.

to 0.83 for PS and ES and 0.70 to 0.78 for PSS. For all vendors, the accuracy of PS and ES was similar, whereas PSS demonstrated lower discrimination capacity ($p < 0.05$). Transmural scars limited to 1 segment (surrounded by normal myocardium) demonstrated higher strain values (-21.6 ± 1.8) than segments with transmural scar that had 2 or more transmural scar neighbors (-0.8 ± 4.6) (Figure 6).

The ability of PSI to distinguish between segments with and without scar was also different among vendors ($p < 0.05$) and ranged from poor to excellent (AUC between 0.68 and 0.85) (Figure 7). All vendor software had significantly more difficulty detecting scars in the basal segments ($p < 0.05$) (Figure 8). If scar was defined according to echocardiographic criteria only instead of CMR LGE, the detection of scar by strain parameters was found to be more accurate in all vendors ($p < 0.05$) (Figure 9).

DISCUSSION

The purpose of the present study was to compare the ability and accuracy to detect abnormal regional myocardial function among 6 vendor-specific and 2 independent strain software tools. We chose myocardial infarct scar as a model of regional dysfunction because it can be defined by an external gold standard method (CMR LGE). To avoid uncertainties in infarct border zones and to minimize the impact of segmentation misalignment between modalities, only segments with full transmural scar and segments free of scar were considered for the analysis.

The main findings of our study are as follows: 1) all vendors measured lower strain values in segments with scar than in segments free of scar; 2) the strain difference between scar and no-scar segments differed significantly among vendors; 3) the ability to distinguish scarred and nonscarred segments differs significantly between vendors; 4) scars located in the basal segments were most difficult to detect; and 5) PSI, PS, and ES were the best parameters to detect scar, whereas PSS performed less well.

SCAR AND REGIONAL DEFORMATION. The presence of transmural scar implies loss of contractile function and a reduction of systolic deformation. Accordingly, in our study, strain values were significantly lower in scarred segments with all vendor software, which is in agreement with previous studies (18,19). Although only segments with transmural scar were considered, a considerable degree of systolic deformation was still measured in the scarred segments (Figure 3). This can be explained in part by mechanical interaction

FIGURE 4 Average Values of PSI in Nonscarred and Scarred Segments

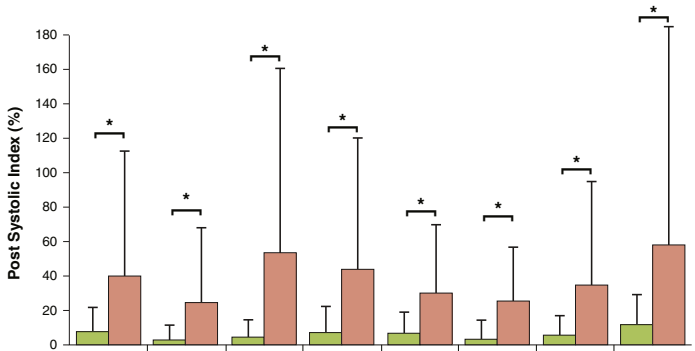

	Hitachi	Esaote	GE	Samsung	Siemens	Toshiba	Epsilon	TOMTEC
No scar	7.7	3.0	4.4	7.5	7.0	3.7	5.6	11.8
Scar	40.2	24.8	53.3	43.9	29.9	25.0	34.8	57.9

All vendors measured a significantly lower PSI (*$p < 0.05$). PSI = post-systolic index.

between the scar tissue and the surrounding myocardium. Tethering forces induce passive deformation, which is biggest in small scars and lowest in the middle of a large scar region. Figure 6 demonstrates that a 1-segment transmural scar can hardly be detected by deformation measurements, because (passive) deformation of the tissue is similar to normal myocardium. It is further supported by the finding that scar definition by visual analysis of echocardiographic images leads to better scar

FIGURE 5 ROC Curves for PS Strain, ES Strain, and PSS Showing the Ability of Each Vendor to Discriminate Between Segments With and Without Transmural Scar as Identified by CMR LGE

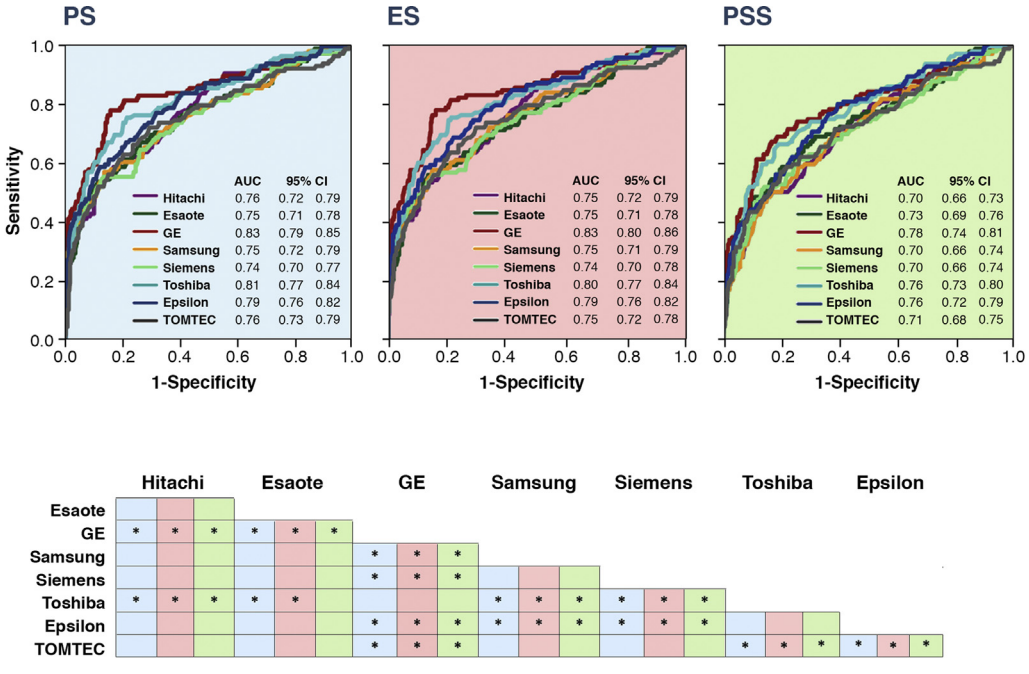

The respective area under the curve (AUC) and 95% confidence intervals (CI) for each vendor are listed in the tables inside the graphs. The table below the graphs shows significant differences in AUC values among vendors (*$p < 0.05$), where PS is represented in **blue**, ES is represented in **pink**, and PSS is represented in **green**. ROC = receiver-operating characteristic; other abbreviations as in Figures 1 and 2.

detection results (higher AUC values) by strain measurements than if CMR LGE is used as the gold standard for scar definition (Figure 9 vs. Figure 5). This is understandable, because the visual echocardiographic analysis considers predominantly functional abnormalities (which are also measured by strain parameters), whereas CMR LGE reflects histological changes in the myocardium.

ABILITY TO DETECT REGIONAL DYSFUNCTION. Nevertheless, the strain difference between scarred and nonscarred segments differed significantly between vendors (Figure 3). We interpret a high difference as a higher fidelity of the software to follow local deformation, a property that is presumably related to the amount of spatial smoothing in the tracking algorithm. Figure 6 shows that a scar that extends over more than 2 segments can lead to clearly abnormal values if the software has a good ability to detect local functional abnormality.

SCAR DETECTION BY STRAIN PARAMETERS. The ability to discriminate between segments with and without scar was at least acceptable in all software packages. Nevertheless, significant differences were observed among vendors, with AUC values for PS and ES between 0.74 and 0.83 (Figure 5). PSI, a parameter that combines both PS and PSS with the intention of describing properties of the curve shape, had the best results, but AUC values showed an even wider range between 0.68 and 0.85 (Figure 7). We presume that these strain parameters are affected by a combination of technical characteristics such as spatial smoothing, temporal smoothing, and local tracking fidelity, as well as image quality.

It was surprising that all vendors had difficulty detecting basal scars (Figure 8). This result could be related in part to the fact that most scar segments were in the apex, where scars stretch over several segments, which makes the likelihood for tethering effects by surrounding normal myocardium lowest. Furthermore, the quality of speckle tracking in the basal region was lowest, which might also contribute to worse distinction between scar and nonscar segments. However, we also noted that the difference between the software performance in the basal and apical regions differed between vendors, with some having reasonable results in all LV levels and others only performing well in the apex.

STUDY LIMITATIONS. In the present study, we compared only endocardial strain measurements, because those were the only strain component that could be provided by all vendors. To what extent an analysis of midwall strain would generate different results remains to be determined.

FIGURE 6 Average Segmental Strain Value in a Scar Segment, Depending on the Number of Surrounding Scar Segments

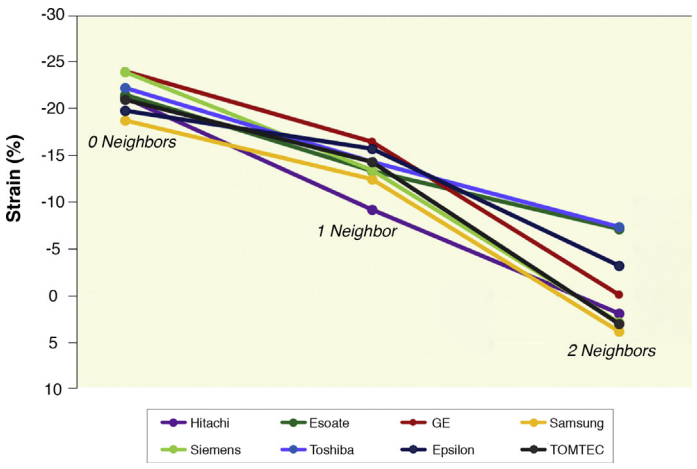

Note the impossibility of detecting a single-segment scar by strain imaging. Bigger scars lead to reduced longitudinal strain. If the scar extent exceeds 2 segments, differences between software solutions become more apparent.

In our study, we used infarct scar as a model of regional myocardial dysfunction. Other regional pathology, such as dyssynchrony in dilated cardiomyopathy, might present a different spectrum of challenges for a software package (thinner walls, more focus on temporal resolution, less focus on

FIGURE 7 ROC Curves for Each Vendor for PSI

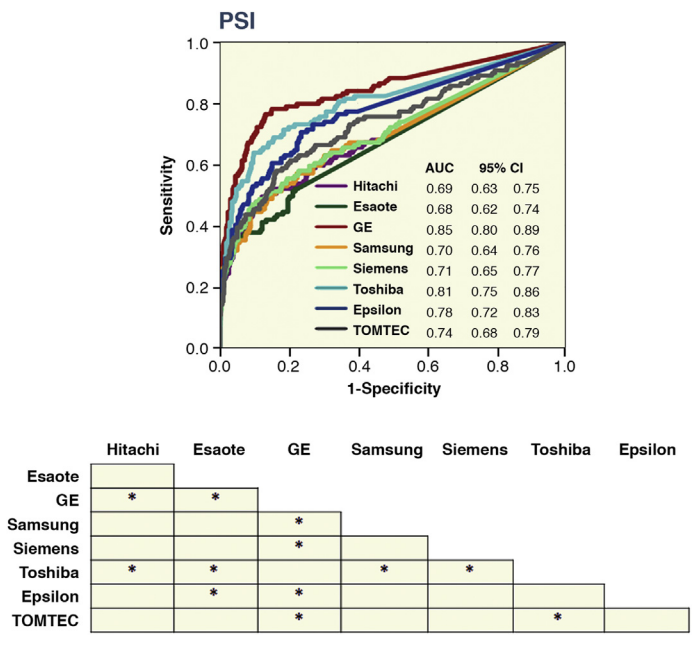

Refer to Figure 5 for a detailed description. *$p < 0.05$.

FIGURE 8 ROC Curves, AUC, and 95% CI for PS Strain Indicating the Ability of Each Vendor to Discriminate Between Segments With and Without Transmural Scar Separated by Scar Location

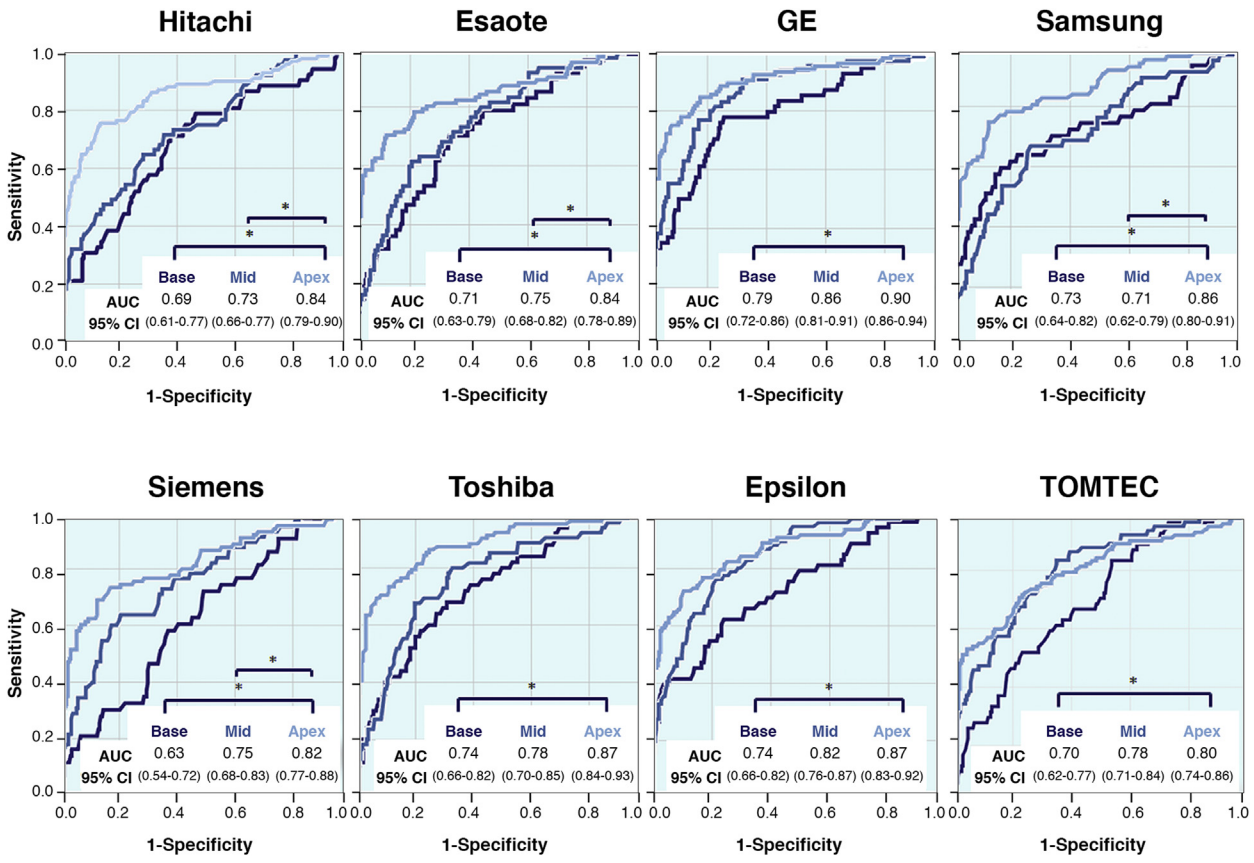

Basal **(dark blue)**, midventricular **(lighter blue)**, and apical **(lightest blue)** scars. Note that all vendors could identify scars significantly better in the apex than at the base (*$p < 0.05$). Abbreviations as in Figure 5.

FIGURE 9 Same Display as Figure 5 but Using the Visual Echocardiography–Based Scar Reading as Gold Standard Instead of the CMR-LGE–Based Scar Definition

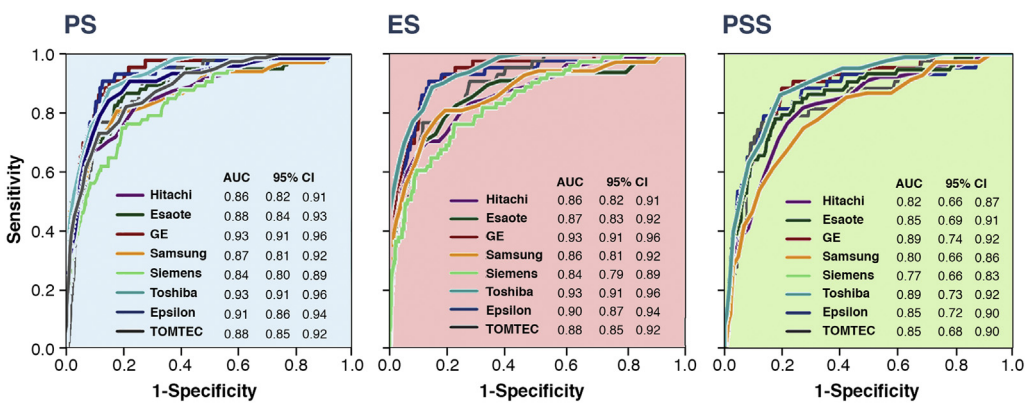

All AUC values were significantly better than those shown in Figure 5. *$p < 0.05$.

spatial resolution) and might lead to slightly differing results. We believe, however, that the possibility of using an external gold standard method (CMR LGE) for the definition of scar location and extent made our study more objective, which outweighs its potential disadvantages.

CONCLUSIONS

In contrast to global strain measurements, which are highly reproducible and also comparable among vendors (6), the ability and accuracy of detecting regional function abnormalities of the LV differ significantly among vendors. This implies that the technical characteristics of the tested software solutions have a considerable impact on the measurement results. Further standardization and pre-release testing, potentially including hardware or software phantoms, is needed to make regional strain analysis a clinically reliable tool that can produce interchangeable results regardless of the software used.

APPENDIX

This paper is published on behalf of the EACVI-ASE-Industry Standardization Task Force, chaired by Luigi P. Badano, Padua (EACVI), and James D. Thomas, Chicago (ASE), and the participating companies, represented by: Jamie Hamilton (Epsilon), Stefano Pedri (Esaote), Peter Lysyansky (GE), Gunnar Hansen (GE), Yasuhiro Ito (Hitachi), Tomoaki Chono (Hitachi), Jane Vogel (Philips), David Prater (Philips), Sungwook Park (Samsung), Jin Yong Lee (Samsung), Helene Houle (Siemens), Bogdan Georgescu (Siemens), Rolf Baumann (TOMTEC), Bernhard Mumm (TOMTEC), Yashuhiko Abe (Toshiba), and Willem Gorissen (Toshiba).

ADDRESS FOR CORRESPONDENCE: Prof. Dr. Jens-Uwe Voigt, Department of Cardiovascular Diseases, University Hospital Gasthuisberg, Herestraat 49, 3000 Leuven, Belgium. E-mail: jens-uwe.voigt@uzleuven.be.

PERSPECTIVES

COMPETENCY IN MEDICAL KNOWLEDGE: In this study, we have tested the accuracy of 6 vendor-specific and 2 independent software packages for strain analysis to identify scarred myocardial segments. Our results indicate there is a significant difference in performance between vendors. Moreover, the localization of the scar and the number of adjacent affected neighbors were shown to influence the ability of the software packages to depict scars.

TRANSLATIONAL OUTLOOK: The fidelity of regional myocardial function assessment by means of segmental longitudinal strain measurements not only depends on type, localization, and extent of the abnormality but also has relevant vendor-specific differences. As of today, a perfect match of good software, good image quality, and careful post-processing and data interpretation with pathophysiologic understanding is still mandatory for meaningful clinical conclusions, which leaves little tolerance for the small imperfections in image acquisition and post-processing, as well as operator skills, that unavoidably exist in daily practice. Although global longitudinal strain has reached a level of development at which it can be safely recommended for clinical use, further improvements in the robustness of regional strain measurements would be desirable to make this great tool more feasible in daily practice.

REFERENCES

1. Stankovic I, Prinz C, Ciarka A, et al. Relationship of visually assessed apical rocking and septal flash to response and long-term survival following cardiac resynchronization therapy (PREDICT-CRT). Eur Heart J Cardiovasc Imaging 2016;17:262–9.

2. Scott PA, Morgan JM, Carroll N, et al. The extent of left ventricular scar quantified by late gadolinium enhancement MRI is associated with spontaneous ventricular arrhythmias in patients with coronary artery disease and implantable cardioverter-defibrillators. Circ Arrhythm Electrophysiol 2011;4:324–30.

3. Chan J, Khafagi F, Young A, Cowan B, Thompson C, Marwick T. Impact of coronary revascularization and transmural extent of scar on regional left ventricular remodelling. Eur Heart J 2008;29:1608–17.

4. Kwon DH, Halley CM, Carrigan TP, et al. Extent of left ventricular scar predicts outcomes in ischemic cardiomyopathy patients with significantly reduced systolic function: a delayed hyperenhancement cardiac magnetic resonance study. J Am Coll Cardiol Img 2009;2:34–44.

5. Amundsen BH, Helle-Valle T, Edvardsen T, et al. Noninvasive myocardial strain measurement by speckle tracking echocardiography: validation against sonomicrometry and tagged magnetic resonance imaging. J Am Coll Cardiol 2006;47:789–93.

6. Farsalinos KE, Daraban AM, Ünlü S, Thomas JD, Badano LP, Voigt JU. Head-to-head comparison of global longitudinal strain measurements among nine different vendors: the EACVI/ASE Inter-Vendor Comparison Study. J Am Soc Echocardiogr 2015;28:1171–81.

7. Tennant R, Wiggers C. The effect of coronary occlusion on myocardial contraction. Am J Physiol 1935;112:351.

8. Jurcut R, Pappas CJ, Masci PG, et al. Detection of regional myocardial dysfunction in patients with acute myocardial infarction using velocity vector imaging. J Am Soc Echocardiogr 2008;21:879–86.

9. Arnold MF, Voigt JU, Kukulski T, Wranne B, Sutherland GR, Hatle L. Does atrioventricular ring motion always distinguish constriction from restriction? A Doppler myocardial imaging study. J Am Soc Echocardiogr 2001;14:391–5.

10. Becker M, Hoffmann R, Kühl HP, et al. Analysis of myocardial deformation based on ultrasonic pixel tracking to determine transmurality in chronic myocardial infarction. Eur Heart J 2006; 27:2560–6.

11. Gjesdal O, Hopp E, Vartdal T, et al. Global longitudinal strain measured by two-dimensional speckle tracking echocardiography is closely related to myocardial infarct size in chronic ischaemic heart disease. Clin Sci (Lond) 2007;113: 287–96.

12. Sjøli B, Ørn S, Grenne B, Ihlen H, Edvardsen T, Brunvand H. Diagnostic capability and reproducibility of strain by Doppler and by speckle tracking in patients with acute myocardial infarction. J Am Coll Cardiol Img 2009;2:24–33.

13. Sun JP, Niu J, Chou D, Chuang HH, et al. Alterations of regional myocardial function in a swine model of myocardial infarction assessed by echocardiographic 2-dimensional strain imaging. J Am Soc Echocardiogr 2007; 20:498–504.

14. Aarsaether E, Rösner A, Straumbotn E, Busund R. Peak longitudinal strain most accurately reflects myocardial segmental viability following acute myocardial infarction: an experimental study in open-chest pigs. J Cardiovasc Ultrasound 2012; 10:23.

15. Lang RM, Badano LP, Mor-Avi V, et al. Recommendations for cardiac chamber quantification by echocardiography in adults: an update from the American Society of Echocardiography and the European Association of Cardiovascular Imaging [published correction appears in Eur Heart J Cardiovasc Imaging 2016;17:412 and Eur Heart J Cardiovasc Imaging 2016;17:969]. Eur Heart J Cardiovasc Imaging 2015;16:233–70.

16. Hosmer DW, Lemeshow S. Applied Logistic Regression. 2nd ed. Wiley; 2000:156–64.

17. DeLong ER, DeLong DM, Clarke-Pearson DL. Comparing the areas under two or more correlated receiver operating characteristic curves: a nonparametric approach. Biometrics 1988;44: 837–45.

18. Rösner A, Avenarius D, Malm S, Iqbal A, Bijnens B, Schirmer H. Severe regional myocardial dysfunction by stress echocardiography does not predict the presence of transmural scarring in chronic coronary artery disease. Eur Heart J Cardiovasc Imaging 2015;16:1074–81.

19. Cimino S, Canali E, Petronilli V, et al. Global and regional longitudinal strain assessed by two-dimensional speckle tracking echocardiography identifies early myocardial dysfunction and transmural extent of myocardial scar in patients with acute ST elevation myocardial infarction and relatively preserved LV function. Eur Heart J Cardiovasc Imaging 2013;14:805–11.

KEY WORDS intervendor differences, longitudinal strain, scar detection

APPENDIX For supplemental figures, please see the online version of this paper.